ADVANCED FUNCTIONAL MATERIALS
www.afm-journal.de

www.MaterialsViews.com

A Chemical Display: Generating Animations by Controlled Diffusion from Porous Voxels

*Yevgeniy V. Kalinin, Shivendra Pandey, Jinpyo Hong, and David H. Gracias**

The concept of utilizing precisely patterned and chemically loaded 3D porous containers akin to chemical voxels to enable dynamic visual patterns via spatial and temporal control of both local and global chemical release is described. Using numerical simulations and experiments, it is shown how variations in porosity, volume, shape, and relative positioning of the chemical voxels can be used to control the types of images that are formed with control in both space and time. Moving images are generated via controlled chemical release from an array of voxels to create an animation of a running man thereby illustrating proof-of-concept for a chemical display.

1. Introduction

Present-day display technologies such as liquid crystal displays, flexible displays, printable electronic displays, electronic paper displays, conformable displays, and wearable displays have become ubiquitous.[1–5] However in all these existing displays, the information displayed by individual pixels is not stored in the pixels themselves but instead sent to the pixels from an external source, typically through wired interfaces.[6,7] Such interfaces which are required to transmit information and address individual pixels can make displays fairly complex, and the electrical power required to operate them can limit utility of these devices.[8] There also exists a technological gap between processes used in conventional media such as painting or printing and those used to create electronic displays. In printing technologies, for instance, once information is sent to the printer to be printed on paper, the dynamic aspect of the information is lost. Hence, printers are only capable of producing static images, with the exception of lenticular printing, where multiple patterns are printed on the same image and a change of the observation angle of the printed image alters the displayed pattern.[9] Here, we describe a new approach for generating moving visual images where the information to be displayed is geometrically encoded in the pixels themselves and the pixels can be dispensed using a variety of techniques such as manual dispensation or nozzle-based printing approaches amenable to both rigid and flexible substrates.

Our approach is inspired by concepts from the field of controlled release wherein particles and devices have been developed and used to release chemicals often drugs, with precise temporal characteristics.[10–19] Controlled release can be achieved in a continuous or pulsatile form, either spontaneously by diffusion[11,12] or in response to various stimuli such as pH,[20,21] temperature,[22–24] electric current,[25] magnetic field,[26] ultrasound,[27] and light radiation.[28,29] In addition to temporal control, recent studies using anisotropic or patterned particles have demonstrated chemical release with spatial variations as well.[30–33] Chemical diffusion has also been used to generate wave-like reaction diffusion patterns and to actuate microstructures.[34–37] In our approach, we also utilize controlled diffusion from chemical sources but importantly, we show that by tuning the characteristics of the sources themselves as well as their relative spatial arrangement, we can generate well-defined animations. Drawing an analogy to digital display technology, we refer to these sources as chemical voxels, and to our knowledge this is the first demonstration of the concept of a chemical display.

We emphasize that while we certainly do not expect chemical displays to replace electronic devices entirely, we note that there are numerous advantages of our approach that could lead to new capabilities for dynamic display technology of relevance to visual, scientific, or biological applications. Chemical displays do not require any wiring, back-end interfaces, interconnects, batteries, or external power sources. The chemical voxels can be dispensed manually or via printing modalities both on rigid and flexible substrates and either in 2D or 3D to generate a variety of moving images on a variety of media, making it possible to create animations with conventional artistic techniques. The voxels can be loaded with chemicals multiple times and hence are reusable. There is considerable versatility and tunability in the time scale of the image especially if images need to be generated over long times. Further, as we show, it is possible to design specific moving images in silico using simulations and that these designs correlate well with experiments, allowing for a rational and software enabled design of moving images in the display. We note that in order to create moving images via chemical release, it is necessary to control the concentration of the chemical in both space and time, both locally at each voxel as well as over the entire image. Importantly, we

Dr. Y. V. Kalinin,[+] Dr. S. Pandey,[++] J. Hong,
Prof. D. H. Gracias
Department of Chemical and Biomolecular Engineering
The Johns Hopkins University
3400 N. Charles St., Baltimore, MD 21218, USA
E-mail: dgracias@jhu.edu

[+]Present address: IBM T. J. Watson Research Center, 1101 Kitchawan Rd., Yorktown Heights, NY 10598, USA
[++]Present address: Intel Corporation, 2501 NW 229th Avenue, Hillsboro, OR 97124, USA

DOI: 10.1002/adfm.201500281

show that both the concentration of chemical and timing (start, peak, and end of the chemical release) can be controlled via manipulation of the characteristics of the porous voxels. Consequently, the essential components of our approach require: a) a high throughput strategy to synthesize chemical voxels in the form of capsules or containers with well-defined volume, shape, and porosity; b) a strategy to dispense and arrange the voxels into well-ordered arrays; and c) design criterion for programmed chemical release with both local and global control based on numerical simulations. We envision that a wide range of chemical voxels such as porous capsules, microgel particles, or reservoir systems could be utilized. Of these, polymer- and gel-based particles can be readily mass-produced in a relatively inexpensive manner but they offer limited control over directional release.[38–40] In our demonstration, we utilize self-folding polyhedral voxels which feature a high degree of control over shape, volume, pore size, surface chemistry, and distribution in all three dimensions. Hence, they serve as a model chemical voxel system to illustrate the concept of a chemical display via controlled chemical release.

2. Results and Discussions

2.1. Numerical Simulations to Control Chemical Diffusion from Voxels

To illustrate control over the timing of chemical release via variation in porosity and shape of the voxel we consider a cube with porous walls (**Figure 1**a). When the porous cubic voxel filled with a chemical is placed into a stationary diffusion medium, the chemical starts diffusing through the pores on the surface. The temporal characteristics of the chemical release, such as its duration of release, timings of start, peak, and end can be controlled via geometric design parameters such as porosity, shape, and volume of the voxels. We define the "start" of the chemical release as the time when chemical starts coming out and its concentration in the vicinity of the voxel is one-half (1/2) of the maximal value. We define the "peak" as the time when the concentration in the vicinity is maximal and the "end" as the time when the concentration of the chemical reaches one-half (1/2) of its maximal value in the vicinity of the voxel (Figure 1b). The use of the (1/2) factor in our definition of "start" and "end" is arbitrary; we could as well have chosen any other reasonable number, such as (1/10) which would lead to a larger temporal separation between peaks of chemical release from multiple voxels. It should be noted that the decay in chemical concentration occurs exponentially and thus never fully reaches a zero value. A typical spatial profile of the chemical concentration around a cubic voxel in a stationary diffusion medium is shown in Figure S1 (Supporting Information). Our simulations suggest that the separation of peaks can be controlled by varying pore sizes and volumes of the voxels (Figure 1b–f). Larger pores result in faster release of chemicals in the vicinity of the voxel and shorten the duration of chemical release. An important feature of our work is the ability to generate a moving image and to this end we observe that it is possible to synchronize the release times from different chemical voxels by varying the pore size and volume of the voxels, so that, for example, some voxels will

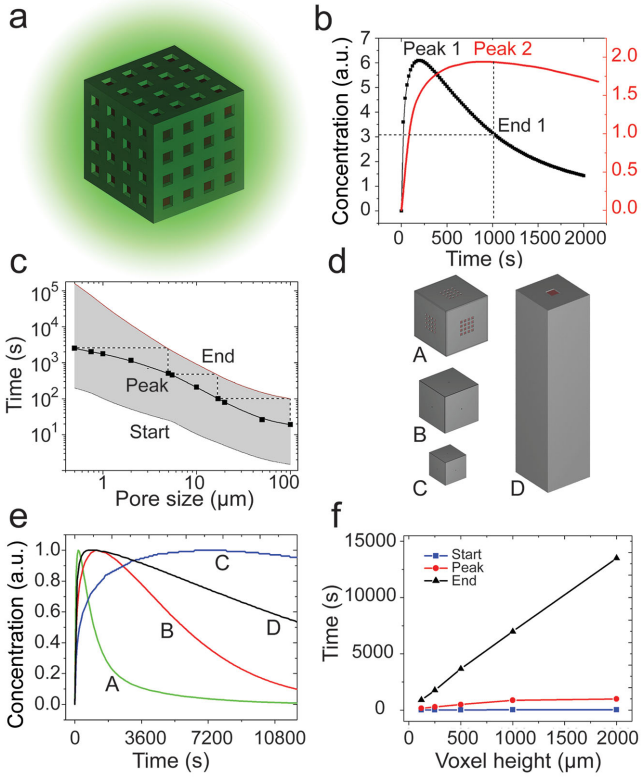

Figure 1. Numerical simulation results demonstrating temporal control over chemical release from chemical voxels with different shapes, sizes, and pore characteristics. a) Schematic illustration of chemical diffusion from a cubic voxel. b) Plot of the typical variation of chemical concentration outside of the voxel as a function of time. The temporal characteristics are determined by the voxel geometry (size and shape) and its porosity. Black line corresponds to diffusion from a 500 μm size cubic voxel with a single 100 μm pore on each face, and red line corresponds to a 500 μm size cubic chemical voxel with a single 20 μm size pore on each face. The temporal characteristics of chemical release can be controlled by varying the pore size in such a way that when the chemical release from one chemical voxel ends ("End 1," $t \approx 1000$ s), the release from the other voxel reaches the peak ("Peak 2," $t \approx 1000$ s). c) Plot of the time of chemical release as a function of pore size. The start, peak, and end points of chemical release are plotted for a 500 μm size cubic chemical voxel. The dashed lines in the plot illustrate the procedure for synchronizing release times from voxels with different pore sizes. For example, in this plot, when the chemical release from a voxel with 100 μm size pore ends, the release from a voxel with 20 μm size pore reaches the peak. This way we can "preprogram" when a given voxel would become visible and when it would fade away. d) Images of voxels with various time release characteristics: (A) is a 500 μm size cubic chemical voxel with a 4×4 array of 25 μm pores on each face, (B) is a 400 μm size cubic chemical voxel with a 17 μm pore on each face, (C) is a 250 μm size cubic chemical voxel with a 3 μm pore on each face, and (D) is a parallelepiped with dimensions $2000 \times 500 \times 500$ μm with a single 100 μm pore. e) Numerical simulation plot of chemical concentration as a function of time for the voxels shown in (d). f) Time of chemical release plotted as a function of voxel volume. Voxels have same pores and cross-section (500 μm × 500 μm) with varying heights. It shows that we can control the duration of chemical release by using voxels with different volumes.

only start releasing chemicals when other voxels have released almost all of their content (Figure 1c). This approach can be utilized for "programming" various time-dependent chemical

patterns by placing precisely designed voxels in the immediate vicinity of each other. Since the duration of the chemical release depends on pore size and volume, we can use voxels of different geometry with different pore characteristics to control the separation of peaks and the duration of chemical release as illustrated in simulation results shown in Figure 1d–f.

2.2. Design of an Animation Using Simulations

In this paper, we demonstrate the concept of a chemical display by arranging chemical voxels of different volumes, pore sizes, and chemical concentrations in an array to generate moving frames of a "running man." The animation was first designed using simulations and then validated in experiments. As in conventional animations, we broke up the moving image of the running man into a sequence of three static images or frames and performed numerical simulations for appropriate arrangements of cube shape voxels with three different volumes, pore sizes, and chemical concentrations to generate three frames (**Figure 2**). In order to control the voxel's start, peak, and end timings, the voxel volume and pore size were varied. Our simulations suggest that a moving image from left to right can be generated by arranging chemical voxels with decreasing volume, decreasing pore size, and increasing concentration from left to right. Thus, the frame on the left should be constructed using voxels with the largest volume, largest pore size, and lowest chemical concentration while the one on the right should be constructed with voxels of the smallest volume, smallest pore size, and highest chemical concentration. This arrangement is done to control the duration of chemical release for the three frames of the "running man" figure with their peaks well separated. As time goes by, the chemical in the voxels of the first frame are depleted (reaches half of the maximal concentration in vicinity) while the concentration of the chemical for second frame is maximum. The same process repeats during generation of the third frame.

Thus, our simulations suggest that moving images can be generated by discretization of frames and arrangement of appropriately designed voxels in terms of their physical dimensions, porosity, and loaded chemical concentrations. To create a single animation, the frames can be arranged either in the same location or on top of each other.

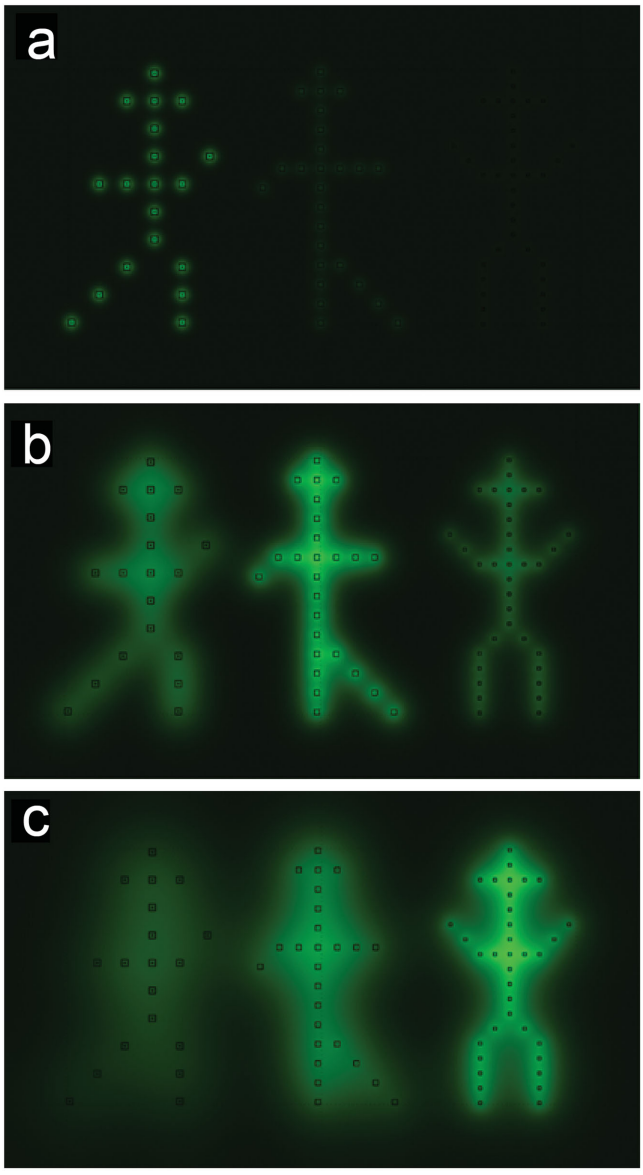

Figure 2. Simulation results showing time-dependent images of the frames of a "running man." a–c) Sequential emergence of three frames of a running man from left to right. The frames are composed of voxels with decreasing volume (from left to right the cubic voxels are 500, 400, and 250 μm in size) with decreasing pore size (from left to right the pores are 100, 17, and 3 μm in size) and increasing chemical concentration of fluorescein (from left to right the fluorescein concentration was 2×10^{-3}, 4×10^{-3}, and 15×10^{-3} M).

2.3. Dispensation of Chemical Voxels on Rigid and Flexible Substrates

In order to validate this concept experimentally, we used fluorescein-loaded cubic voxels, which were attached to glass substrates. First, we fabricated the chemical voxels using surface tension driven self-assembly, by a process that has been detailed previously.[41,42] Briefly, prepatterned planar templates of a desired shape are defined on a sacrificial layer using photolithography with metal frames and solder hinges. The templates are released by dissolving the sacrificial layer and self-assemble on heating into porous polyhedra with well-sealed edges due to surface energy minimization of the molten solder hinges. We fabricated cubic voxels of various sizes with various pore characteristics and arranged them on a glass slide to represent fixed chemical sources or chemical voxels for the generation of three frames of a running man in a chemical display (**Figure 3**). To highlight the use of our methodology with conventional artistic media we also show that the voxels can be printed with fairly high throughput. By using a voxel-loaded pipette we were able to write the shape of a house (**Figure 4**a,b). While our approach was done by hand it could as well be implemented by automated nozzle-based computer controlled printing techniques allowing arrangements in both 2D and 3D.[43–45] From

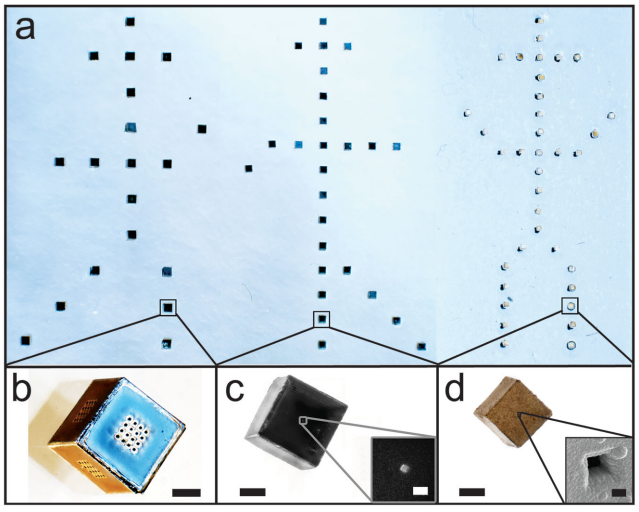

Figure 3. Ordered arrangements of chemical voxels used to fabricate the chemical display. a) Top view of the chemical voxels arranged on a glass slide that represents the first, second, and third frames of a "running man." From left to right, each frame is formed by a single voxel type: 500 μm size voxels with a 4 × 4 array of 25 μm pores on each face, 400 μm size voxels with a single 17 μm size pore on each face, and 250 μm size voxels with a single 3 μm size pore on each face. All three frames were imaged separately and then stitched together. b–d) The corresponding cubes used to create the chemical voxels for the frames from left to right shown in (a). The inset in (c) is a zoomed image of a 17 μm size pore and the inset in (d) is a zoomed SEM image of a 3 μm size pore. Scale bars are 100 μm for (b–d), 30 μm for the inset in (c), and 2 μm for the inset in (d).

a functional standpoint, as shown in Figure 4c–f, voxels can be arranged both on rigid and flexible substrates highlighting the ability to create displays by chemical diffusion on a variety of substrates in 2D, curved and folded geometries. It is important to note that it can be challenging to create displays using conventional electronic pixels on such media due to the incompatibility of these material substrates with the high temperatures and vacuum-based processes used in microelectronic fabrication.[46–49]

2.4. Experimental Validation of the Animation

We used fluorescein-loaded voxels to visualize the image; alternate chemicals with different colors could also be utilized. As designed, the first frame appears at the time when the fluorescence intensity of fluorescein released from the chemical voxels constituting this frame reaches its peak. When the fluorescence intensity of the first frame decreases to the half of its maximal value, the fluorescence intensity of the voxels in second frame reaches the peak and thus the second frame becomes visible. Similarly, when the fluorescence intensity of the chemical voxels in the second frame reduces to half of its maximal value, the third frame becomes visible. Hence, the three frames appear one after the other from left to right in agreement with simulations (**Figure 5**). Details of fabrication of voxels, loading of chemicals, arrangement methods, and imaging of chemical diffusion are given in the Supporting Information.

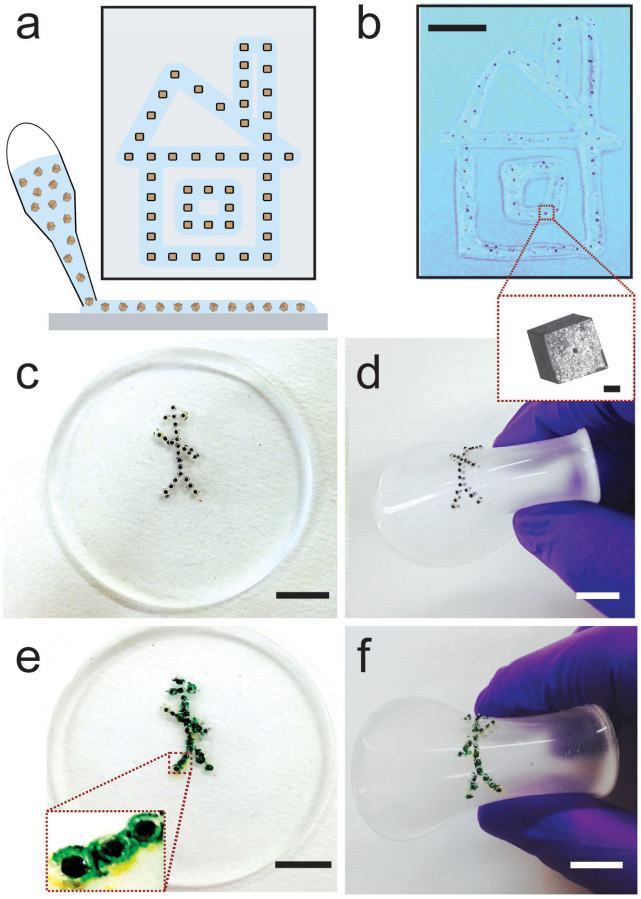

Figure 4. Dispensing voxels on rigid and flexible surfaces. a) Schematic illustration of the dispensation of chemical voxels using a nozzle-based approach to create the shape of a house on a glass slide. b) Optical image depicting voxels written using pipette filled with agarose gel in the shape of a house. The agarose gel serves as a diffusion medium to visualize chemicals released from the voxels. The zoomed inset is an optical image of a single cube shaped chemical voxel. c,d) Optical images of dodecahedron-shaped chemical voxels arranged on a polydimethylsiloxane (PDMS) surface to illustrate an artistic design of a man on a flexible substrate. e,f) Optical images showing chemical diffusion from dye loaded chemical voxels on the PDMS surface. Scale bars: 1 cm for (b–f) and 100 μm for the inset in (b).

3. Conclusions

Our studies suggest a proof-of-concept for the fabrication and operation of a chemical display. The resolution of the display is based on the size of the chemical voxels as well as their spacing. In comparison to conventional electronic displays, while no sharp "pixel" boundaries can be formed by a diffusion process, the gradients of chemical concentration in the vicinity of the pores are very high (Figure S1, Supporting Information). Accordingly, the size of the chemical "pixel" is comparable to the size of the voxel that created it. High chemical gradients also allow the pixels to remain visible even as the chemical background concentration increases. This is essential for the voxels that are programmed to become visible at later times as more and more chemical voxels release their chemical content. When working with multiple voxels at close spacing, a chemical

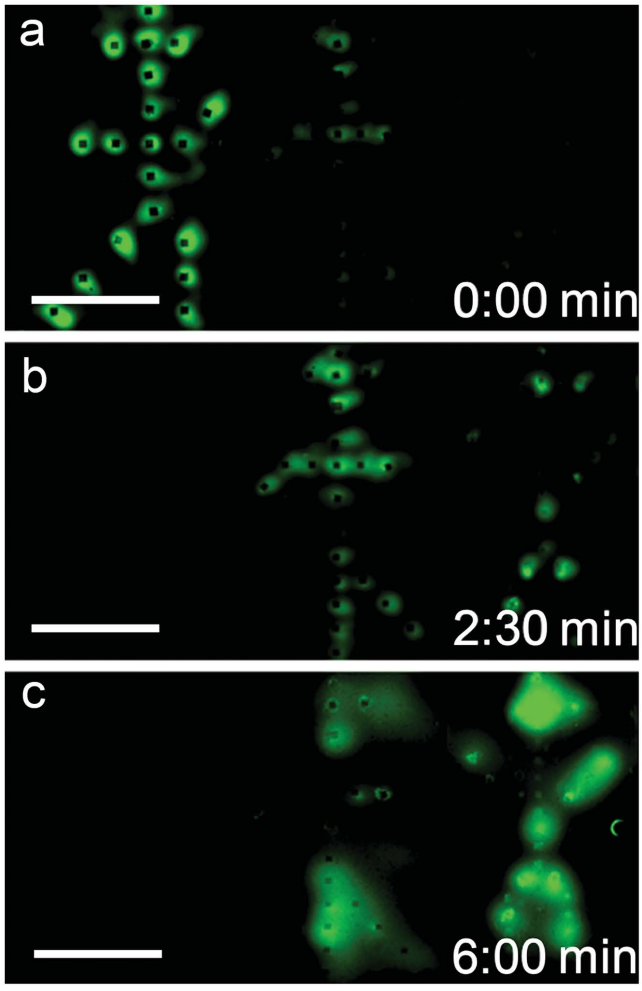

Figure 5. Experimental demonstration of a chemical display depicting a man running from left to right. a–c) Experimental results showing time-dependent images of the frames of a running man via fluorescein diffusion from chemical voxels in a diffusion medium consisting of glycerol, ethanol, and water in a ratio of 2:1:1 (v/v). All three frames were imaged separately at the same time and then the frames were stitched together. a) Initially only the first frame becomes visible. b) After 2:30 min, the first frame completely fades away and the second frame becomes visible. c) Finally at time 6:00 min, the first two frames fade away and the third frame becomes visible. Scale bars: 1 cm.

voxel will alter the concentration in the vicinity of its neighbors that has some effect on the chemical release from the neighboring voxels; these effects were taken into account in the simulation of the running man.

In terms of the size of the voxels, we note that a variety of nanostructured liposomes, microgel particles, or even similar self-folded containers already exist at 100 nm length scales, which is a size far smaller than the 10 μm size range of conventional toner particles used in 600 dots per inch (dpi) printing technologies.[50,51] As noted earlier, higher precision approaches such as traditional ink-jet or 3D printing could also be utilized on unpatterned or patterned substrates.[52,53] Prepatterned substrates could also aid in registry. For example, previously we have shown how egg-crate like substrates could be used to orient polyhedra[54] suggesting that anisotropic and oriented diffusive patterns from local voxels could also be utilized. Further, arranging chemical voxels on a preexisting grid ensures a precise orientation relative to the substrate and thus local voxel diffusion can be optimized for a specified layout. In this arrangement, the reusable array of voxels which releases the fluorescent dye via diffusion behaves as other displays, such as electrophoretic spheres (also known as E Ink[55]) or a prototype microfluidic display.[56] The main difference between the chemical display presented here and other techniques is the absence of external connections or interfaces in our case. Here, the timing information is encoded in the voxels themselves and it is programmed via engineering the volume, porosity, and chemical concentration of the voxels. We note that while our demonstration was shown using diffusion from passive voxels, it could as well utilize existing stimuli-responsive voxels such as those responsive to light, radio frequency, or ultrasound allowing on-demand or remotely controlled animations.[27,57] Further, the substrates with chemical voxels printed on them can be reused by either simply submerging them in the solutions of the dyes, creating a microfluidic interface, or by relying on chemical reactions; these features are important from a recycling and sustainability standpoint. Finally, additional time and color variability can be added by utilizing multiple chemicals, such as ones with lower diffusion coefficients.

In addition to media applications, we envision that the methodology could also be used in biotechnology and bioengineering to create programmable chemical patterns such as dynamic gradients to direct cellular behaviors.[58] In the case of a single chemical release from multiple containers, this technique can be used to create complicated release profiles[59] in a manner similar to the Fourier decomposition. Alternatively, the technique can be used to time the release of multiple chemicals such as growth factors, where sequential release is known to be critical for the formation of organized tissues and organs.[60] The proposed methodology would complement existing techniques,[28,61–63] while allowing for precise timing of the release by relying only on the shape and size variations of the voxels.

4. Experimental Section

Numerical Simulations: Numerical simulations were performed using COMSOL Multiphysics (COMSOL, Inc.). It was assumed that the voxels were surrounded by a 4 mm thick stationary medium and solutions were sought to the time-dependent diffusion equation in stationary medium in the absence of chemical reactions as described previously.[58] Simulation results such as those shown in Figure 2 were obtained by plotting the concentration field in a plane parallel to the plane of the voxels and offset from it by 600 μm. Photobleaching of the fluorescent dye was not taken into account in the simulations. In addition, when calculating chemical release from individual voxels zero boundary conditions were assumed thus neglecting possible chemical interactions between voxels. Such interactions were taken into account in simulations of chemical release from ordered voxel arrangements.

Fabrication of Voxels: In this study, the voxels were fabricated in a high throughput manner using a surface tension–driven self-assembly technique in which prepatterned 2D templates of voxels self-fold and self-seal due to minimization of surface energy of the molten hinges.[41,42] Planar templates of voxels using AutoCAD were designed and were printed on transparency film to make photomasks. These

photomasks were utilized for photolithography, and consequently electroplating and wet etching techniques to pattern 2D panels and solder hinges. The hinged templates from the substrate were released by dissolving an underlying sacrificial layer and the templates were heated to 200 °C, above the melting point of the solder to self-assemble templates into perfectly closed and sealed voxels. In order to decrease the pore size below the resolution of the transparency film photomasks, which was 8 μm in this case, gold (Au) was deposited by electroplating after self-assembly. Due to the electrically conductive nature of the polyhedra, the gold deposited on both the inside and outside of the cubes and the final size of the pores was reduced by the amount of gold electroplated.[19]

Positioning of the Voxel Arrays and Chemical Loading: Voxels can either be positioned manually or by nozzle-based printing methods. In order to write a house shape (Figure 4b), ≈200 cube shaped voxels were added in a 2 mL (1% w/v) agarose gel and mixed well using a pipette. A disposable transfer pipette was used (Fisherbrand; Catalog No. 13-711-7M) to dispense the voxels and write a shape of house on a glass slide. The gel solidified in 5–7 min at room temperature. To create the design of a man on a flexible surface (Figure 4c-f), the elastomer base and curing agent (Dow Corning Sylgard 184 Silicone Elastomer Kit) were first mixed in a ratio of 10:1 (w/w) and put in a desiccator to remove bubbles. After removing the bubbles, it was cured at 65 °C for 2 h to prepare a flexible polydimethylsiloxane (PDMS) substrate. Then, 300 μm sized dodecahedron shaped voxels were positioned manually on the PDMS substrate and attached with an adhesive (Gorilla Glue). These voxels were loaded by covering them with a green color liquid dye (McCormick Food Color & Egg Dye) and placing the substrate in a desiccator for 10 min to speed up the loading process. The excess dye was removed by rinsing the voxels with distilled water and the excess was dried by wiping with KimWipes. Similarly, for the animation of a running man (Figure 5), the cubic voxels were positioned manually to form three frames of a running man figure and attached them on glass slides using an adhesive (Gorilla Glue). Arrayed voxels were loaded with fluorescein (Sigma-Aldrich; Fluorescein Sodium Salt, Catalog No. 231-791-2) by soaking them in aqueous solutions overnight. In the case of voxels with small pores, the voxels were placed in a desiccator to remove air bubbles and speed up the loading process. It was also found that the addition of a Pluronic P-123 surfactant at 0.1% (w/v) facilitated voxel loading with chemicals more readily but the surfactant led to the voxel detachment from the glass slides so its use was discontinued. The concentrations of chemicals loaded in the voxels were calculated in accordance with the numerical simulations (Figure 2). To generate the animation shown in Figure 5, solutions of fluorescein with different concentrations were utilized, 2×10^{-3} M aqueous solution for the first frame, 4×10^{-3} M for the second frame, and 15×10^{-3} M fluorescein solution for the third frame, from left to right.

Chemical Diffusion and Imaging: In order to generate the moving images of the running man (Figure 5), loaded chemical voxels were rinsed briefly with water and were gently wiped to remove any excess fluorescein that remained on the outer surface of the voxels. The arrayed voxels were placed in a 4 mm tall PDMS chamber and the display was activated by gently pouring a mix of glycerol, ethyl alcohol, and water in a ratio of 2:1:1 (v/v) onto the chemical voxels. A schematic of the experimental setup is shown in Figure S2 (Supporting Information). The diffusion of fluorescein under a fluorescence microscope was imaged. Each frame was imaged separately but at the same time and then stitched together to make an animation of three frames thus illustrating a running man figure from left to right. The voxels were used and reused for image formation over ten times.

Supporting Information

Supporting Information is available from the Wiley Online Library or from the author.

Acknowledgements

Y.V.K. and S.P. contributed equally to this work. This research work was supported by the National Science Foundation Grant No. CBET-1066898.

Received: January 22, 2015
Revised: April 7, 2015
Published online: May 28, 2015

[1] Y. Chen, J. Au, P. Kazlas, A. Ritenour, H. Gates, M. McCreary, *Nature* **2003**, *423*, 136.
[2] S. W. Stephenson, D. M. Johnson, J. I. Kilburn, X.-D. Mi, C. M. Rankin, R. G. Capurso, *SID Int. Symp. Dig. Tech. Pap.* **2004**, *35*, 774.
[3] R. Sakurai, S. Ohno, S.-I. Kita, Y. Masuda, R. Hattori, *SID Int. Symp. Tech. Pap.* **2006**, *37*, 1922.
[4] Y. Chen, K. Denis, P. Kazlas, P. Drzaic, *SID Int. Symp. Dig. Tech. Pap.* **2001**, *32*, 157.
[5] G. A. Freeman, D. H. Freeman, *US Patent No. 5,931,764*, **1999**.
[6] J. A. Castellano, *Handbook of Display Technology* Academic, San Diego **1992**.
[7] G. P. Crawford, *Flexible Flat Panel Displays* Wiley, New York **2005**.
[8] H. Zhang, M. Sakakura, H. Kuwabara, *U.S. Patent 6,243,155*, **2001**.
[9] R. B. Johnson, G. A. Jacobsen, *SPIE Proc.* **2005**, *5874*, 587406.
[10] K. E. Uhrich, S. M. Cannizzaro, R. S. Langer, K. M. Shakesheff, *Chem. Rev.* **1999**, *99*, 3181.
[11] H. M. Creque, R. Langer, J. Folkman, *Diabetes* **1980**, *29*, 37.
[12] N. A. Peppas, R. Gurny, E. Doelker, P. Buri, *J. Membr. Sci.* **1980**, *7*, 241.
[13] T. P. Richardson, M. C. Peters, A. B. Ennett, D. J. Mooney, *Nat. Biotechnol.* **2001**, *19*, 1029.
[14] A. Rösler, G. W. M. Vandermeulen, H.-A. Klok, *Adv. Drug Delivery Rev.* **2001**, *53*, 95.
[15] D. A. Edwards, J. Hanes, G. Caponetti, J. Hrkach, A. Ben-Jebria, M. L. Eskew, J. Mintzes, D. Deaver, N. Lotan, R. Langer, *Science* **1997**, *276*, 1868.
[16] I. C. Kwon, Y. H. Bae, S. W. Kim, *Nature* **1991**, *354*, 291.
[17] R. Langer, *Chem. Eng. Commun.* **1980**, *6*, 1.
[18] E. Leo, A. Scatturin, E. Vighi, A. Dalpiaz, *J. Nanosci. Nanotechnol.* **2006**, *6*, 3070.
[19] C. L. Randall, T. G. Leong, N. Bassik, D. H. Gracias, *Adv. Drug Delivery Rev.* **2007**, *59*, 1547.
[20] V. Patel, M. M. Amiji, *Pharm. Res.* **1996**, *13*, 588.
[21] R. A. Siegel, M. Falamarzian, B. A. Firestone, B. C. Moxley, *J. Controlled Release* **1988**, *8*, 179.
[22] A. Gutowska, Y. H. Bae, J. Feijen, S. W. Kim, *J. Controlled Release* **1992**, *22*, 95.
[23] A. S. Huffman, A. Afrassiabi, L. C. Dong, *J. Controlled Release* **1986**, *4*, 213.
[24] A. Serres, M. Baudyš, S. W. Kim, *Pharm. Res.* **1996**, *13*, 196.
[25] A. D'Emanuele, J. N. Staniforth, *Pharm. Res.* **1991**, *8*, 913.
[26] D. S. T. Hsieh, R. Langer, J. Folkman, *Proc. Natl. Acad. Sci. U.S.A.* **1981**, *78*, 1863.
[27] J. Kost, K. Leong, R. Langer, *Proc. Natl. Acad. Sci. U.S.A.* **1989**, *86*, 7663.
[28] E. Mathiowitz, M. D. Cohen, *J. Membr. Sci.* **1989**, *40*, 1.
[29] E. Mathiowitz, A. Raziel, M. D. Cohen, E. Fischer, *J. Appl. Polym. Sci.* **1981**, *26*, 809.
[30] T. Leong, Z. Gu, T. Koh, D. H. Gracias, *J. Am. Chem. Soc.* **2006**, *128*, 11336.
[31] Y. V. Kalinin, A. Murali, D. H. Gracias, *R. Soc. Chem. Adv.* **2012**, *2*, 9707.

[32] K. M. Ainslie, C. M. Kraning, T. A. Desai, *Lab Chip* **2008**, *8*, 1042.
[33] S. L. Tao, T. A. Desai, *Adv. Mater.* **2005**, *17*, 1625.
[34] S. Maeda, Y. Hara, T. Sakai, R. Yoshida, S. Hashimoto, *Adv. Mater.* **2007**, *19*, 3480.
[35] V. Petrov, V. Gáspár, J. Masere, K. Showalter, *Nature* **1993**, *361*, 240.
[36] R. Yoshida, T. Takahashi, T. Yamaguchi, H. Ichijo, *J. Am. Chem. Soc.* **1996**, *118*, 5134.
[37] A. N. Zaikin, A. M. Zhabotinsky, *Nature* **1970**, *225*, 535.
[38] R. P. Batycky, J. Hanes, R. Langer, D. A. Edwards, *J. Pharm. Sci.* **1997**, *86*, 1464.
[39] X. Zhao, S. Jain, H. B. Larman, S. Gonzalez, D. J. Irvine, *Biomaterials* **2005**, *26*, 5048.
[40] K. J. Pekarek, J. S. Jacob, E. Mathiowitz, *Nature* **1994**, *367*, 258.
[41] T. G. Leong, P. A. Lester, T. L. Koh, E. K. Call, D. H. Gracias, *Langmuir* **2007**, *23*, 8747.
[42] S. Pandey, E. Gultepe, D. H. Gracias, *J. Vis. Exp.* **2013**, *72*, e50022.
[43] H. P. Le, *J. Imaging Sci. Technol.* **1998**, *42*, 49.
[44] H. Lipson, M. Kurman, *Fabricated: The New World of 3D Printing* Wiley, New York **2013**.
[45] M. S. Mannoor, Z. Jiang, T. James, Y. L. Kong, K. A. Malatesta, W. O. Soboyejo, N. Verma, D. H. Gracias, M. C. McAlpine, *Nano Lett.* **2013**, *13*, 2634.
[46] S.-I. Park, Y. Xiong, R.-H. Kim, P. Elvikis, M. Meitl, D.-H. Kim, J. Wu, J. Yoon, C.-J. Yu, Z. Liu, Y. Huang, K.-C. Hwang, P. Ferreira, X. Li, K. Choquette, J. A. Rogers, *Science* **2009**, *325*, 977.
[47] H. O. Jacobs, A. R. Tao, A. Schwartz, D. H. Gracias, G. M. Whitesides, *Science* **2002**, *296*, 323.
[48] C. Yu, Y. Li, X. Zhang, X. Huang, V. Malyarchuk, S. Wang, Y. Shi, L. Gao, Y. Su, Y. Zhang, *Proc. Natl. Acad. Sci. U.S.A.* **2014**, *111*, 12998.
[49] Q. Wang, G. R. Gossweiler, S. L. Craig, X. Zhao, *Nat. Commun.* **2014**, *5*, 4899.
[50] V. Wood, M. J. Panzer, J. Chen, M. S. Bradley, J. E. Halpert, M. G. Bawendi, V. Bulović, *Adv. Mater.* **2009**, *21*, 2151.
[51] H.-H. Lee, K.-S. Chou, K.-C. Huang, *Nanotechnology* **2005**, *16*, 2436.
[52] P. Calvert, *Chem. Mater.* **2001**, *13*, 3299.
[53] K. Seki, Y. Onozawa, S. Inukai, N. Ono, *US Patent 8,308,271*, **2012**.
[54] C. L. Randall, Y. V. Kalinin, M. Jamal, T. Manohar, D. H. Gracias, *Lab Chip* **2011**, *11*, 127.
[55] B. Comiskey, J. D. Albert, H. Yoshizawa, J. Jacobson, *Nature* **1998**, *394*, 253.
[56] P. Drzaic, *Nat. Photonics* **2009**, *3*, 248.
[57] a) H. Ye, C. L. Randall, T. G. Leong, D. A. Slanac, E. K. Call, D. H. Gracias, *Angew. Chem. Int. Ed.* **2007**, *46*, 4991; b) H. Ye, C. L. Randall, T. G. Leong, D. A. Slanac, E. K. Call, D. H. Gracias, *Angew. Chem.* **2007**, *119*, 5079.
[58] a) Y. V. Kalinin, J. S. Randhawa, D. H. Gracias, *Angew. Chem. Int. Ed.* **2011**, *50*, 2549; b) Y. V. Kalinin, J. S. Randhawa, D. H. Gracias, *Angew. Chem.* **2011**, *123*, 2597.
[59] F.-M. Chen, M. Zhang, Z.-F. Wu, *Biomaterials* **2010**, *31*, 6279.
[60] R. R. Chen, E. A. Silva, W. W. Yuen, D. J. Mooney, *Pharm. Res.* **2007**, *24*, 258.
[61] K. C. Wood, H. F. Chuang, R. D. Batten, D. M. Lynn, P. T. Hammond, *Proc. Natl. Acad. Sci. U.S.A.* **2006**, *103*, 10207.
[62] M. S. Aw, J. Addai-Mensah, D. Losic, *Chem. Commun.* **2012**, *48*, 3348.
[63] J. H. Prescott, T. J. Krieger, S. Lipka, M. A. Staples, *Pharm. Res.* **2007**, *24*, 125.